would have been recorded and compared with the CA and CS mass spectra described above. It was also attempted to make the 2-norbornyl anion, by dissociative electron detachment or by reaction of various norbornyl derivatives with OH^- in the mass spectrometer's ion source. Had a significant flux of $[C_7H_{11}]^-$ ions been produced, then their collision-induced charge reversal mass spectrum[24] would have been investigated. Finally, the neutralization-reionization mass spectra[25] of the various $[C_7H_{11}]^+$ ions were recorded, using Xe as the charge exchange gas and He as reionization gas.[26] All $[C_7H_{11}]^+$ produced intermediate free radicals of sufficient stability to be collisionally reionized, but the mass spectra proved to contain no clear structural distinctions.

Experimental Section

Unimolecular ion fragmentations and the various collision-induced events were observed using a VG Analytical ZAB-2F mass spectrometer under conditions referenced in the text or as described elsewhere.[27] Appearance energies were measured using an apparatus comprising an electrostatic electron monochromator[28] together with a quadrupole mass analyzer and minicomputer data system.[29] Compounds were of research grade and used without further purification. *exo*-2-Norbornyl iodide was prepared by treating norbornene with HI at −78 °C.

Acknowledgment. M.C.B. acknowledges a Graduate Studentship from the Province of Ontario, and J.L.H. thanks the Natural Sciences and Engineering Research Council of Canada for continuing financial support.

Registry No. 2-Norbornyl cation, 24321-81-1; 2,4-octadiene, 13643-08-8; 2,6-octadiene, 4974-27-0; 3,6-dimethylcyclohexene, 19550-40-4; 1-methylcyclohexene, 591-49-1; norbornane, 279-23-2; 3-ethylcyclopentene, 694-35-9; vinylcyclopentane, 3742-34-5; ethylidenecyclopentane, 2146-37-4; *exo*-2-norbornyl bromide, 2534-77-2; *exo*-2-norbornyl iodide, 30983-85-8; norbornene, 498-66-8.

(23) Burgers, P. C.; Holmes, J. L.; Mommers, A. A.; Szulejko, J. E.; Terlouw, J. K. *Org. Mass Spectrom.* **1984**, *19*, 442.
(24) Bowie, J. H.; Blumenthal, T. *J. Am. Chem. Soc.* **1975**, *97*, 2959.
(25) Danis, P. O.; Wesdemiotis, C.; McLafferty, F. W. *J. Am. Chem. Soc.* **1983**, *105*, 7454.
(26) Terlouw, J. K.; Kieskamp, W. M.; Holmes, J. L.; Mommers, A. A.; Burgers, P. C. *Int. J. Mass Spectrom. Ion Proc.* **1985**, *64*, 245.
(27) Burgers, P. C.; Holmes, J. L.; Szulejko, J. E.; Mommers, A. A.; Terlouw, J. K. *Org. Mass Spectrom.* **1983**, *18*, 254.
(28) Maeda, J.; Semeluk, G. P.; Lossing, F. P. *Int. J. Mass Spectrom. Ion Phys.* **1968**, *1*, 395.
(29) Lossing, F. P.; Traeger, J. C. *Int. J. Mass Spectrom. Ion Phys.* **1976**, *19*, 9.

Dynamic Processes in Crystals Examined through Difference Displacement Parameters ΔU: Pseudo-Jahn–Teller Distortion in *cis*-$Cu^{II}N_4O_2$ Coordination Octahedra

M. Stebler and H. B. Bürgi*

Contribution from the Laboratorium für Chemische und Mineralogische Kristallographie der Universität, CH-3012 Bern, Switzerland. *Received April 28, 1986*

Abstract: Anisotropic displacement parameters ("temperature factors") obtained from routine single-crystal diffraction experiments contain chemically useful information. This is shown for $[Cu^{II}(LL)_2OXO]$ complexes (LL is phenanthroline, bipyridine, or bipyridylamine, OXO is NO_2^-, $HCOO^-$, or CH_3COO^-) which undergo static or dynamic pseudo-Jahn-Teller deformation. Observed displacement parameters reflect this deformation: they agree well with results from model calculations based on a simplified potential energy curve for the deformation.

The primary results from single-crystal diffraction experiments are long lists of atomic positional and displacement ("thermal") parameters. It is generally accepted that positional parameters are a reliable source of information on molecular structure. The attitude of chemists and crystallographers toward the information contained in displacement parameters is ambiguous and may be characterized as one of negligent pessimism which is changing only slowly toward cautious optimism.

Several recent studies justify this change: The rigid body model of molecular motion in crystals as derived from displacement parameters[1] has been generalized to allow treatment of molecules with internal flexibility.[2-5] The chemical or physical significance of motional characteristics derived from displacement parameters has been tested by comparing results from diffraction experiments with results from other methods.[5,6] The comparisons indicate that significant information on internal molecular motion may be obtained even from routine structure determinations. Here this conclusion is exemplified by analyzing literature data for $[Cu^{II}(LL)_2OXO]$ complexes, some of which undergo automerization in the solid state (Figure 1). It will be shown how the structural changes occurring during this process may be obtained from observed harmonic, anisotropic displacement parameters.

Crystal and molecular structures have been published for several compounds of general composition $[Cu^{II}(LL)_2OXO]Y$ (Table I and V). LL is one of the bidentate ligands 2,2′-bipyridine (bipy), 1,10-phenanthroline (phen), or 2,2′-bipyridylamine (bipyam). OXO is bidentate nitrite (ONO^-), nitrate (ONO_2^-), acetate (CH_3COO^-), or formate ($HCOO^-$). Y is a noncoordinating anion (NO_3^-, BF_4^-, ClO_4^-). The complex cations show a wide spectrum of octahedral coordination geometries. Cu–N distances trans to each other are between 1.97 and 2.01 Å (Cu–N3, Cu–N4) and Cu–N distances trans to O's between 2.02 and 2.18 Å (Cu–N1,

(1) (a) Schomaker, V.; Trueblood, K. N. *Acta Crystallogr., Sect. B: Struct. Crystallogr. Cryst. Chem.* 1968, *B24*, 63. (b) Cruickshank, D. W. J. *Acta Crystallogr.* **1956**, *9*, 754–756.
(2) Johnson, C. K. In *Crystallographic Computing*; Ahmed, F. R. Ed.; Munksgaard, Copenhagen, 1970.
(3) (a) Schomaker, V.; Trueblood, K. N. *Acta Crystallogr., Sect A: Found Crystallogr.* **1984**, *A40*, C-339. (b) Dunitz, J. D.; White, D. N. J. *Acta Crystallogr., Sect. A: Cryst. Phys., Diffr., Theor. Gen. Crystallogr.* **1973**, *A29*, 93. (c) Trueblood, K. N.; Dunitz, J. D. *Acta Crystallogr., Sect. B: Struct. Sci.* **1983**, *B39*, 120.
(4) He, X. M.; Craven, B. M. *Acta Crystallogr., Sect. A: Found Crystallogr.* **1985**, *A41*, 244.
(5) (a) Bürgi, H. B. *Trans. Am. Crystallogr. Assoc.* **1984**, *20*, 61. (b) Ammeter, J. H.; Bürgi, H. B.; Gamp, E.; Meyer-Sandrin, V.; Jensen, W. P. *Inorg. Chem.* **1979**, *18*, 733. (c) Chandrasekhar, K.; Bürgi, H. B. *Acta Crystallogr., Sect. B: Struct. Sci.* **1984**, *B40*, 387–397.
(6) (a) Brock, C. P.; Dunitz, J. D. *Acta Crystallogr., Sect. B: Struct. Crystallogr. Cryst. Chem.* **1982**, *B38*, 2218. (b) Bonadeo, H.; Burgos, E. *Acta Crystallogr., Sect. A: Cryst. Phys., Diffr., Theor. Gen. Crystallogr.* **1982**, *A38*, 29. (c) Gramaccioli, C. M.; Filippini, G. *Acta Crystallogr., Sect A: Found. Crystallogr.* **1983**, *A39*, 784.

0002-7863/87/1509-1395$01.50/0 © 1987 American Chemical Society

Table I. Listing of Structure Determinations

compound	code	space group	site symm	T,[a] K	ref[b]
$[Cu(bipy)_2ONO]BF_4$	[CuO1]	$P2_1/n$	1	RT	1
$[Cu(bipy)_2ONO]NO_3$	[CuO2]	$P2_1/n$	1	RT	2
$[Cu(bipy)_2ONO]NO_3$	[CuO3]	$P2_1/n$	1	298	3, 4
$[Cu(bipy)_2ONO]NO_3$	[CuO4]	$P2_1/n$	1	165	3, 4
$[Cu(bipy)_2ONO]NO_3$	[CuO5]	$P2_1/n$	1	100	5
$[Cu(bipy)_2ONO]NO_3$	[CuO6]	$P2_1/n$	1	20	5
$[Cu(phen)_2ONO]BF_4$	[CuO7]	$P\bar{1}$	1	RT	6
$[Cu(bipyam)_2ONO]BF_4$	[CuO8]	$P2_1/n$	1	RT	7
$[Cu(bipyam)_2ONO]NO_2$	[CuO9]	$Pccn$	2	RT	8
$[Cu(bipy)_2NO_3]NO_3*H_2O$	[Cu11]	$P\bar{1}$	1	RT	9
$[Cu(bipy)_2NO_3]*H_2O$	[Cu12]	$P\bar{1}$	1	RT	10
$[Cu(bipy)_2NO_3]PF_6$	[Cu13]	$P\bar{1}$	1	RT	11
$[Cu(bipy)_2CH_3COO]BF_4$	[Cu21]	$P2_1/c$	1	RT	12
$[Cu(bipy)_2CH_3COO]ClO_4*H_2O$	[Cu22]	$P\bar{1}$	1	RT	12
$[Cu(phen)_2CH_3COO]BF_4$	[Cu23]	$P\bar{1}$	1	296	11, 13, 14
$[Cu(phen)_2CH_3COO]ClO_4$	[Cu24]	$P2_1/c$	1	298	13, 15
$[Cu(phen)_2CH_3COO]ClO_4$	[Cu25]	$P2_1/c$	1	173	15
$[Cu(phen)_2CH_3]ClO_4*2H_2O$	[Cu26]	$P2/c$	2	RT	11, 13, 16
$[Cu(phen)_2CH_3COO]BF_4*2H_2O$	[Cu27]	$P2/_c$	2	RT	6, 13
$[Cu(phen)_2CH_3COO]NO_3*2H_2O$	[Cu28]	$P\bar{1}$	1	RT	11, 16
$[Cu(bipyam)_2CH_3COO]NO_3$	[Cu29]	$P2_1/c$	1	RT	7
$[Cu(bipy)_2HCOO]BF_4*0.5H_2O$	[Cu31]	$P\bar{1}$	1	RT	17
$[Cu(phen)_2HCOO]BF_4$	[Cu32]	$C2/c$	2	RT	11
$[Cu(phen)_2HCOO]ClO_4$	[Cu33]	$C2/c$	2	298	18, 19
$[Cu(bipyam)_2HCOO]BF_4$	[Cu34]	$P2_1/c$	1	RT	11

[a] RT is room temperature. RT was assumed if no temperature was specified. [b] For references see Table V.

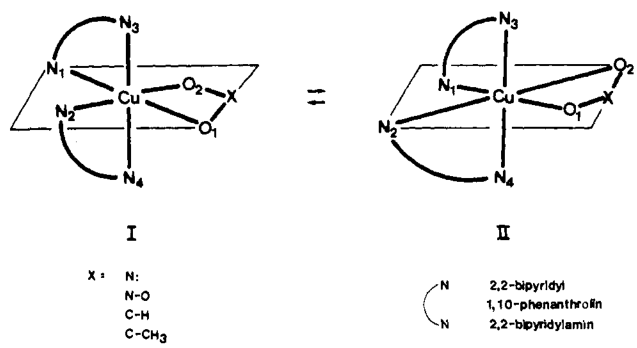

Figure 1. Pseudooctahedral coordination in $[Cu^{II}(LL)_2OXO]Y$ complexes. Two isomers with different but equivalent pseudo-Jahn–Teller distortions are shown (I, II).

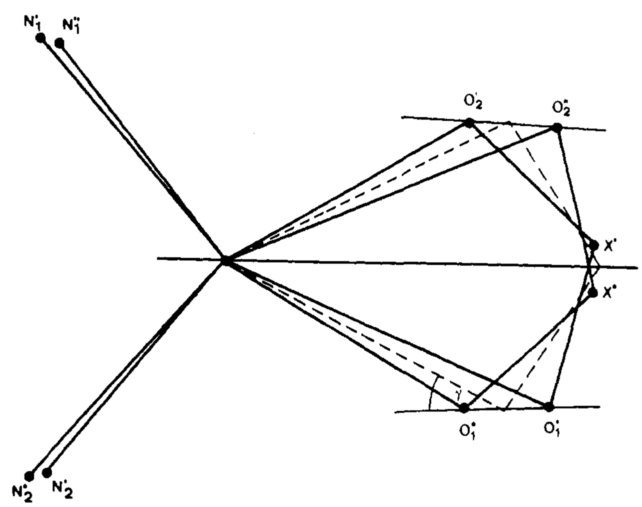

Figure 2. Model of disorder in the equatorial plane of cis CuN_4O_2 ions. Pseudo-Jahn–Teller distorted molecules I (primed atoms) and II (doubly primed atoms) are shown. The dotted lines indicate mean O and X positions for $P = 0.5$.

Cu–N2). Cu–O distances cover a substantially larger range, 1.97–2.88 Å. There is a tendency for Cu–N1 and Cu–O1 to be shorter than Cu–N2 and Cu–O2, respectively, or vice versa (Figure 1, Table II). Differences in Cu–N distances trans to O range from 0 to ~0.2 Å, in Cu–O distances from 0 to ~0.9 Å.[7,8] Small differences are invariably accompanied by unusually anisotropic mean-square displacement parameters of the oxygen atoms. The largest displacement is approximately in the direction of the Cu–O internuclear vector. It is composed of two contributions: One reflecting static or dynamic disorder of O1 and O2 over two positions[9] (primed and doubly primed, Figure 2), and another one resulting from the usual intra- and intermolecular motion in the crystal. The mean-square displacements of Cu result from intra- and intermolecular motion only. The difference ΔU in mean-square displacement between oxygen and copper should therefore represent an approximate measure of the effects of disorder. The difference is small if the two positions have very different populations, i.e., if disorder is small and distances Cu–O1 and Cu–O2 are very different. The difference is maximal if the two populations are equal, i.e., if disorder is maximal and apparent distances Cu–O1 and Cu–O2 are equal. In the general case, ΔU may be shown to depend on the negative square of the difference in the apparent Cu–O1 and Cu–O2 distances (Figure 4).

The paper is structured as follows. After giving details of the data retrieval, the electronic structure of $[Cu^{II}(LL)_2OXO]^+$ complexes is reviewed insofar as it is responsible for the observed disorder phenomenon. Then a model of the effect of disorder on structural and displacement parameters is developed and compared with observed difference displacement parameters.

Data Retrieval. Data retrieval from the Cambridge Crystallographic Data Base[10] and from authors of unpublished results yielded 25 data sets pertaining to 19 different compounds of

(7) Walsh, A.; Walsh, B.; Murphy, B.; Hathaway, B. J. *Acta Crystallogr., Sect. B: Struct. Crystallogr. Cryst. Chem.* **1981**, *B37*, 1512.
(8) Hathaway, B. J. *Coord. Chem. Rev.* **1983**, *52*, 87–169.
(9) Simmons, C. J.; Seff, K.; Clifford, F.; Hathaway, B. J. *Acta Crystallogr., Sect. C: Cryst. Struct. Commun.* **1983**, *C39*, 1360.
(10) Allen, F. H.; Bellard, S.; Brice, M. D.; Cartwright, B. A.; Doubleday, A.; Higgs, H.; Hummelink, T.; Hummelink-Peters, B. G.; Kennard, O.; Motherwell, W. D. S.; Rodgers, J. R.; Watson, D. G. *Acta Crystallogr., Sect. B: Struct. Crystallogr. Cryst. Chem.* **1979**, *B35*, 2331.

Table II. Apparent Distances (Å) in *cis*-[Cu(LL)$_2$OXO]Y Complexes[a]

code	Cu-O1	Cu-O2	Cu-N1	Cu-N2	Cu-N3	Cu-N4	Cu···X
[Cu01]	2.1169	2.4623	2.0523	2.1416	1.9900	2.0043	2.7339
[Cu02]	2.2382	2.3289	2.0650	2.1001	1.9810	2.0053	2.7320
[Cu03]	2.2299	2.3200	2.0730	2.0844	1.9794	1.9881	2.7297
[Cu04]	2.2040	2.3509	2.0700	2.0979	1.9839	1.9891	2.7299
[Cu05]	2.1557	2.4145	2.0598	2.1099	1.9870	1.9919	2.7333
[Cu06]	2.0524	2.5364	2.0281	2.1419	1.9825	1.9973	2.7252
[Cu07]	2.0714	2.5974	2.0494	2.1673	1.9987	2.0195	2.7713
[Cu08]	2.1116	2.5513	2.0217	2.1393	1.9845	2.0131	2.7780
[Cu09]	2.0735	2.5504	2.0951	2.0951	2.0079	2.0079	2.6781
[Cu11]	2.3004	2.8318	2.0228	2.0509	1.9734	1.9859	2.9687
[Cu12]	2.2984	2.8178	2.0219	2.0449	1.9841	1.9826	2.9583
[Cu13]	2.1525	2.7460	2.0345	2.1030	1.9813	1.9766	2.8290
[Cu21]	1.9794	2.7842	2.0333	2.2088	1.9948	2.0167	2.7149
[Cu22]	2.0317	2.6476	2.0564	2.1674	1.9712	1.9933	2.6627
[Cu23]	1.9953	2.6706	2.0625	2.2189	2.0095	2.0254	2.6552
[Cu24]	2.2171	2.4204	2.0965	2.1315	1.9905	2.0055	2.6473
[Cu25]	2.1554	2.5279	2.0968	2.1414	2.0018	2.0126	2.6908
[Cu26]	2.2520	2.2520	2.1225	2.1225	1.9985	1.9985	2.6461
[Cu27]	2.2616	2.2615	2.1233	2.1233	2.0004	2.0004	2.6465
[Cu28]	2.1237	2.4478	2.0823	2.1712	2.0003	2.0192	2.6354
[Cu29]	2.0331	2.6726	2.0314	2.1607	2.0082	2.0099	2.6851
[Cu31]	2.0234	2.8691	2.0613	2.1578	1.9777	2.0022	2.7422
[Cu32]	2.363	2.363	2.111	2.111	1.990	1.990	
[Cu33]	2.353	2.353	2.111	2.111			
[Cu34]	2.0015	2.8755	2.0232	2.1663	1.9999	2.0155	2.7464

[a] One ligand contains N1, N3, the other N2, N4.

composition [Cu^{II}(LL)$_2$OXO]Y (Table I). The study covers the literature up to July 1983. Two structure determinations at room temperature have been published for [Cu(bipy)$_2$NO$_3$]NO$_3$·H$_2$O ([Cu11], [Cu12]) and for [Cu(bipy)$_2$ONO]NO$_3$ ([CuO2], CuO3]). For the latter, structural data at four different temperatures ([CuO3]–[CuO6]), for [Cu(phen)$_2$CH$_3$COO]ClO$_4$ at two different temperatures ([Cu24], [Cu25]), are available. No data could be obtained for [Cu(bipy)$_2$ONO]PF$_6$ (cited in ref 6 of Table V). As has been discussed previously,[5c] analysis of atomic displacement parameters should be accompanied by a critical assessment of experimental details, i.e., of the diffraction data and of the models used to intrepret them. Relevant information is summarized as far as available in a table deposited as supplementary material. Most data sets show a conventional R value of ~0.05 and may be considered typical for "routine structure determinations". Resolution is moderate, and effects of absorption and anomalous dispersion would seem to be relatively small; on the whole, very similar scattering factor information has been used in the various structure analyses. It is clear from the table that reporting of experimental details leaves much to be desired. In summary, the data and their interpretation are very similar for all data sets, except for [CuO2] (film data).

Interatomic distances (Table II) and angles were recalculated by using the XRAY76 package of programs;[11] difference displacement parameters ΔU_{obsd} (Table IV) were obtained with the program THMB (version 6; ref 12). Statistical analyses and some graphic representations were obtained with the SAS program package.[13]

Electronic Structure of [Cu^{II}(LL)$_2$OXO]$^+$. The electronic ground state of Cu(II) ions in an octahedral or trigonal field of six chemically equivalent ligands is ^2E, i.e., electronically doubly degenerate. Replacement of one pair of cis coordinated atoms by another pair reduces the symmetry of the ligand field and leads to a splitting of the ^2E state into a ^2A and a ^2B state. If the energy difference between these states is sufficiently small and if there is vibronic coupling with a displacement coordinate of B symmetry,

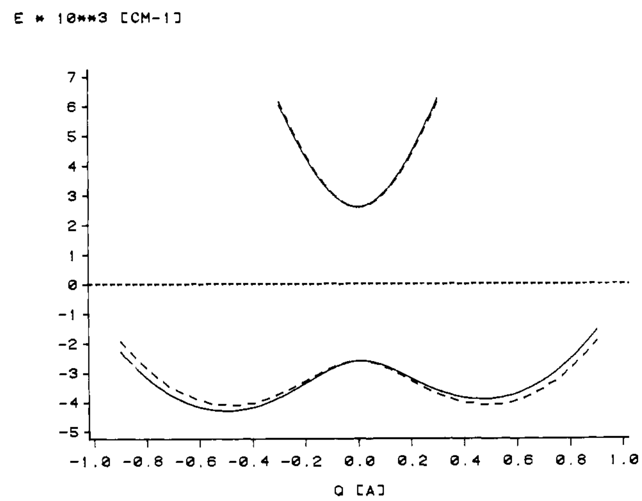

Figure 3. Schematic energy profile for pseudo-Jahn–Teller distortion of [$Cu^{II}N_4O_2$] ions in a symmetric (- - -) and an asymmetric environment (—): upper curves, $E(^2B) = kQ^2/2 + (\Delta^2 + a^2Q^2)^{1/2} + bQ$; lower curves, $E(^2A) = kQ^2/2 - (\Delta^2 + a^2Q^2)^{1/2} + bQ$; numerical values, k = 27 000; a = 14 000; Δ = 2600 cm^{-1} (ref 14); b = 0 for dotted curve; b = 400 cm^{-1} Å^{-1} for solid curve.

the complex distorts, its total energy being lowered in the process (pseudo-Jahn–Teller distortion).[14]

The situation described above is found in [Cu^{II}(LL)$_2$OXO]$^+$ ions with their *cis*-CuN$_4$O$_2$ coordination. Vibronic coupling produces a structural distortion along the approximate coordinate

$$|Q| \approx \{[d(\text{Cu-N1}) - d(\text{Cu-N2})]^2 + [d(\text{Cu-O1}) - d(\text{Cu-O2})]^2\}^{1/2}/\sqrt{2}$$

$Q > 0$ is defined to imply a lengthening of d(Cu–N1) and d(Cu–O1) and a shortening of d(Cu–N2) and d(Cu–O2) by the same amounts; for $Q < 0$ the distortion is reverse (Figure 2). For an isolated ion the lowering in energy is the same for $+Q$ and $-Q$ (Figure 3). The same is true for an ion in a crystal site with a

(11) Stewart, J. M.; Machin, P. A.; Dickinson, C. W.; Ammon, H. L.; Heck, H.; Flack, H. XRAY76 system, Computer Science Center, University of Maryland.
(12) Trueblood, K. N. THMB (version 6) Thermal Motion Analysis, University of California, Los Angeles, 1982.
(13) *SAS User's Guide, 1982 Edition*; SAS Institute Inc.: Cary, NC, 1982.

(14) Simmons, C. J.; Clearfield, A.; Fitzgerald, W.; Tyagi, S.; Hathaway, B. J. *Inorg. Chem.* **1983**, *22*, 2463.

Table III. Difference Displacement Parameters ΔU_{obsd} and esd[a] for *cis*-[Cu(LL)$_2$OXO]Y Compounds[b]

code	ΔUO1 (σ)	ΔUO2 (σ)	ΔUN1 (σ)	ΔUN2 (σ)	ΔUN3 (σ)	ΔUN4 (σ)
[Cu01]	443 (35)	626 (35)	20 (27)	39 (27)	52 (26)	43 (22)
[Cu02]	619 (67)	784 (75)	78 (56)	−35 (46)	71 (69)	−115 (59)
[Cu03]	665 (37)	725 (37)	−37 (24)	−5 (25)	39 (23)	28 (23)
[Cu04]	623 (28)	671 (29)	55 (19)	17 (17)	−24 (13)	−58 (13)
[Cu05]	505 (16)	578 (17)	42 (13)	43 (13)	47 (12)	12 (11)
[Cu06]	39 (9)	62 (9)	8 (11)	26 (11)	51 (10)	50 (10)
[Cu07]	207 (25)	708 (34)	49 (24)	−25 (23)	14 (24)	29 (24)
[Cu08]	138 (28)	230 (41)	−5 (30)	−3 (29)	8 (26)	13 (29)
[Cu09]	63 (77)	418 (95)	34 (80)	3 (67)	−57 (63)	14 (67)
[Cu11]	12 (30)	347 (31)	10 (23)	12 (17)	41 (21)	90 (22)
[Cu12]	90 (36)	348 (41)	89 (32)	58 (30)	64 (24)	72 (28)
[Cu13]	64 (24)	459 (41)	−22 (18)	12 (25)	43 (18)	37 (24)
[Cu21]	8 (28)	250 (33)	12 (33)	3 (34)	9 (32)	13 (35)
[Cu22]	79 (23)	586 (36)	29 (28)	23 (28)	56 (28)	24 (28)
[Cu23]	133 (12)	532 (24)	51 (13)	−24 (13)	42 (13)	39 (13)
[Cu24]	1074 (44)	2388 (58)	13 (28)	−70 (27)	34 (28)	42 (27)
[Cu25]	986 (42)	2361 (61)	26 (16)	−42 (16)	52 (18)	1 (18)
[Cu26]	1170 (12)	1170 (12)	26 (13)	26 (13)	48 (12)	48 (12)
[Cu27]	1131 (46)	1131 (46)	1 (30)	1 (30)	40 (20)	40 (20)
[Cu28]	887 (23)	1094 (29)	65 (18)	31 (17)	24 (12)	52 (18)
[Cu29]	46 (46)	179 (47)	7 (48)	−10 (53)	−3 (46)	39 (45)
[Cu31]	56 (25)	601 (34)	18 (26)	−17 (25)	47 (25)	11 (24)
[Cu32]	1881	1881	14	14	41	41
[Cu33]	1817	1817	16	16		
[Cu34]	−24 (42)	78 (65)	13 (48)	−43 (54)	−6 (48)	38 (50)

[a] In parentheses. [b] $\Delta UO1 = \Delta U_{obsd}$(Cu–O1), $\Delta UN2 = \Delta U_{obsd}$(Cu–N2), etc.

twofold symmetry axis defined by the Cu and mean X positions. For ions in sites with no symmetry the energy of the distorted complex is different for $+Q$ and $-Q$ due to the difference in crystal environment (Figure 3). In the former case distortions $+Q$ and $-Q$ are equally likely. In the latter case the probability of occurrence for the two distorted ions depends on the energy difference ΔE between the two and on temperature. The ratio of the corresponding Boltzmann population factors is

$$P(+Q)/P(-Q) = \exp(-\Delta E/RT)$$

with $P(+Q) + P(-Q) = P + (1 - P) = 1$. Except for $P \approx 0$ or 1 the observed structure will be disordered.

In a seminal contribution[14] Simmons et al. have recently shown how ΔE can be derived from diffraction experiments alone if data at several temperatures are available. Their reasoning forms a basis for discussing effects of disorder on structural parameters as explained in the next section.

Effect of Disorder on Structural and Displacement Parameters. In this section the disorder model used to represent the structures of *cis*-CuN_4O_2 complexes is summarized, and its effects on observed molecular geometry and atomic displacement parameters are analyzed.

In both ordered ($\Delta E >> RT$) and disordered ($\Delta E \sim RT$) structures each O and N atom is represented by a single set of positional and anisotropic displacement parameters (see references in Table V). In disordered structures the positional parameters obtained for O and N must therefore correspond to apparent mean positions and not to the actual positions in the distorted complexes (Figure 2).

The variance of apparent mean structure has been analyzed by principal component analysis on the 18 independent parameters of the fragment [CuN_4OXO]. Results for [Cu(LL)$_2$ONO]$^+$ are discussed here as an example. The nine data sets [CuO1]–[CuO9] were complemented by nine others in which the atomic labels O1, N1, and N3 were interchanged with O2, N2, and N4. Thus for each structure resembling I, the equivalent structure resembling II was added (Figure 1). The symmetrization of the data set ensures a mean structure with C_2 symmetry (Table IVa). Variances are largest for d(Cu–O) and angles O1CuN1 and O2CuN2 indicating that these parameters are the most affected by the transition I $\rightleftarrows$ II (Figure 1). The largest principal component accounts for ~54% of the total correlation in the data (Table IVb). The associated eigenvector is antisymmetric with respect to the twofold axis of the mean structure, i.e., a shortening of d(Cu–O1) by $0.3\sigma[d(\text{Cu–O1})]$ is accompanied by a corresponding lengthening of d(Cu–O2), and an opening of the angle O1CuN1 by 0.3 σ(O1CuN1) is accompanied by a corresponding closing of the angle O2CuN2, etc. The next two components accounting for ~27% of the total correlation come with symmetric eigenvectors. They express changes in bond angles upon shortening or lengthening the Cu to ligand distances. These factors express mainly the variable steric constraints imposed by the different bidentate ligands phen, bipy, and bipyam. According to the usual criteria, the remaining factors with eigenvalues less than 1 are chemically insignificant (only two of these are shown in Table IVb).

From the mean distances and angles (Table IVa) and from the first principal component the geometrical model (Figure 2) for the interconversion I $\rightleftarrows$ II (Figure 1) is constructed. Adding or subtracting to the mean parameters ~1.3 times the respective standard deviations yields a structure that is very similar to the most asymmetric ones ($P \sim 0$ or 1, Table II) and yields estimates of effective (as opposed to apparent) distances. Figure 2 indicates that the disorder, especially in O1 and O2, should affect positional and displacement parameters. The former will correspond to mean position between primed and unprimed atoms, and the latter will be increased in the Cu–O directions by an amount ΔU_{dis} to account for the distribution of O atoms over two positions. The quantities ΔU_{dis} may be estimated along the following lines:[5c] apparent internuclear distances expressed in terms of effective distances are

$$\langle d(\text{Cu–O1})\rangle = Pd(\text{Cu–O1}') + (1 - P)d(\text{Cu–O1}'')$$

$$\langle d(\text{Cu–O2})\rangle = Pd(\text{Cu–O2}') + (1 - P)d(\text{Cu–O2}'')$$

Assuming $d(\text{Cu–O1}') = d(\text{Cu–O2}'')$, $d(\text{Cu–O1}'') = d(\text{Cu–O2}')$ and defining $\Delta d(\text{Cu–O}) \equiv [d(\text{Cu–O}_1') - d(\text{Cu–O}_1'')]/2$, $\langle \Delta d(\text{Cu–O})\rangle \equiv [\langle d(\text{Cu–O}_1)\rangle - \langle d(\text{Cu–O}_2)\rangle]/2$ the following quadratic relation between effective distances, apparent distances, and ΔU_{dis} is obtained

$$\Delta U_{dis} \approx \Delta d^2(\text{Cu–O}) - \langle \Delta d(\text{Cu–O})\rangle^2 \approx 4P(1 - P)\Delta d^2(\text{Cu–O}) \quad (1)$$

In the case of symmetric disorder ($P = 0.5$) this reduces to $\Delta U_{dis} \approx \Delta d^2(\text{Cu–O})$. In the case of no disorder ($P = 1$ or 0) $\Delta U_{dis} = 0$. Note that studies at multiple temperatures may provide an extensive test of eq 1 if P changes with T.

Table IV

(a) Mean Distances, Angles, and Standard Deviations of Populations for $[Cu^{II}(LL)_2ONO]^+$ Complexes

	Cu-O1	Cu-O2	Cu-N1	Cu-N2	Cu-N3	Cu-N4
mean	2.298	2.298	2.088	2.088	1.995	1.995
st dev	0.186	0.186	0.041	0.041	0.012	0.012
	Cu···X	O1CuO2	O1CuN1	O1CuN2	O1CuN3	O1CuN4
mean	2.735	52.9	154.4	102.3	90.5	88.1
st dev	0.028	1.0	6.3	5.7	2.9	2.7
	X-O1	X-O2	O2CuN2	O2CuN1	O2CuN4	O2CuN3
mean	1.241	1.241	154.4	102.3	90.5	88.1
st dev	0.023	0.023	6.3	5.7	2.9	2.7

(b) The Five Largest Principal Components of the Correlation Matrix

eigenvalues	9.68	2.82	1.96	0.94	0.88
eigenvectors	1	2	3	4	5
Cu-O1	−0.304	−0.051	−0.052	−0.030	0.207
Cu-O2	0.304	−0.051	−0.052	−0.030	−0.207
Cu-N1	−0.302	−0.096	−0.035	0.125	−0.177
Cu-N2	0.302	−0.096	−0.035	0.125	0.177
Cu-N3	−0.203	−0.286	−0.337	0.177	−0.183
Cu-N4	0.203	−0.286	−0.337	0.177	0.183
Cu···X	−0.000	−0.374	0.234	−0.707	−0.000
X-O1	0.218	0.125	−0.199	−0.195	0.405
X-O2	−0.218	0.125	−0.199	−0.195	−0.405
O1CuO2	−0.000	0.546	−0.186	0.194	−0.000
O1CuN1	0.288	0.216	−0.046	−0.030	−0.057
O1CuN2	−0.303	0.103	0.001	−0.031	0.053
O1CuN3	0.194	0.187	0.492	0.075	−0.145
O1CuN4	−0.124	−0.282	0.232	0.371	0.448
O2CuN2	−0.288	0.216	−0.046	−0.030	0.057
O2CuN1	0.303	0.103	0.001	−0.031	−0.053
O2CuN4	−0.194	0.187	0.492	0.075	0.145
O2CuN3	0.124	−0.282	0.232	0.371	−0.448

The mean-square amplitude quantity $\Delta\mathbf{U}_{dis}$ may thus be calculated for any disordered case in terms of observable distances alone, namely from $\langle\Delta d(\text{Cu-O})\rangle$ and $\Delta d(\text{Cu-O})$ (obtained from structures with $P = 0$ or 1), and compared to observed values of $\Delta\mathbf{U}_{dis}$. The necessary relationship between $\Delta\mathbf{U}_{dis}$ and observed mean-square displacement parameters, $\mathbf{U}_{obsd}$, will be given in the following section.

Relationship between Calculated and Observed Difference Displacement Parameters U. Harmonic anisotropic displacement parameters measure the mean-square displacement of an atom in a crystal in a given direction. In general, they are represented by a second rank tensor $\mathbf{U}'$ referred to the reciprocal axes of the crystal. After transformation to a molecular cartesian coordinate system, $(\mathbf{U}' \rightarrow \mathbf{U})$ the mean-square displacement $\langle u^2\rangle$ in a particular direction l is obtained from the quadratic form $\langle u^2(\mathrm{l})\rangle = \mathbf{l}^T\mathbf{U}\mathbf{l}$, where $\mathbf{l}$ is a unit vector in the desired direction. The eigenvalues and eigenvectors of $\mathbf{U}$ ($\mathbf{U}'$) define the displacement ellipsoid. Since numerical values of $\mathbf{U}$ have almost disappeared from the printed page of most journals, these ellipsoids have become the main source of information about atomic motion in the crystal for the reader of crystallographic papers. The vivid graphical representation is an insufficient substitute, however, for quantitative analysis.

Observed atomic displacement parameters are conveniently discussed in terms of overall molecular translational and rotational rigid body oscillations on the one hand[1] and internal vibrations on the other.[2-5] Rigid body motion excludes—by definition—unequal displacements of two atoms in a rigid molecule along their internuclear vector. This implies that nonvanishing differences between displacement parameters along internuclear vectors $\mathbf{l}$ are due to intramolecular motion.

$$\Delta\mathbf{U}_{obsd} = \Delta\mathbf{U}_{intra} = \mathbf{l}^T\mathbf{U}_{obsd}(\text{atom 1})\mathbf{l} - \mathbf{l}^T\mathbf{U}_{obsd}(\text{atom 2})\mathbf{l}$$

Such differences are a relatively reliable probe for such motion, because systematic errors in $\mathbf{U}_{obsd}$ tend to cancel on calculating the difference $\Delta\mathbf{U}_{obsd}$.[5c] In the present case $\Delta\mathbf{U}_{obsd}$ is composed of the usual small apmplitude atomic displacement due to bond stretching motions of the distorted cis CuN_4O_2 ion ($\Delta\mathbf{U}(\text{Cu-O})$) and of large amplitude displacements due to pseudo Jahn-Teller distortion ($\Delta\mathbf{U}_{dis}$), i.e.,

$$\Delta\mathbf{U}_{obsd} = \langle\Delta\mathbf{U}_{stretch}\rangle + \Delta\mathbf{U}_{dis}$$

where

$$\langle\Delta\mathbf{U}_{stretch}(\text{Cu-O1})\rangle = P\Delta\mathbf{U}(\text{Cu-O1}') + (1 - P)\Delta\mathbf{U}(\text{Cu-O1}'')$$

$$\langle\Delta\mathbf{U}_{stretch}(\text{Cu-O2})\rangle = P\Delta\mathbf{U}(\text{Cu-O2}') + (1 - P)\Delta\mathbf{U}(\text{Cu-O2}'')$$

Assuming $\Delta\mathbf{U}(\text{Cu-O1}') = \Delta\mathbf{U}(\text{Cu-O2}'') \equiv \Delta\mathbf{U}_l$, $\Delta\mathbf{U}(\text{Cu-O1}'') = \Delta\mathbf{U}(\text{Cu-O2}') \equiv \Delta\mathbf{U}_s$, the following expression is obtained.

$$\Delta\mathbf{U}_{obsd} = (\Delta\mathbf{U}_l + \Delta\mathbf{U}_s)/2 + (\Delta\mathbf{U}_l - \Delta\mathbf{U}_s)/2\cdot \langle\Delta d(\text{Cu-O})\rangle/\Delta d(\text{Cu-O}) + \Delta d^2(\text{Cu-O}) - \langle\Delta d(\text{Cu-O})\rangle^2 \quad (2)$$

This relationship is closely related to eq 1 but differs from it by the addition of terms in $\Delta\mathbf{U}_l$ and $\Delta\mathbf{U}_s$ arising from internal stretching motions not related to the pseudo-Jahn-Teller deformation. Given the above relationship, it would seem of interest to analyze experimental values of $\Delta\mathbf{U}_{obsd}$ for quadratic dependence on $\langle\Delta d(\text{Cu-O})\rangle$ and to estimate the quantities $\Delta d(\text{Cu-O})$, $\Delta\mathbf{U}_l$ and $\mathbf{U}_s$ for an ordered complex.[5]

Analysis of Experimental Values for $\Delta\mathbf{U}_{obsd}$ and $\langle\Delta d(\text{Cu-O})\rangle$. Difference displacement parameters $\Delta\mathbf{U}_{obsd}(\text{Cu-N})$ are of a magnitude expected for intramolecular stretching motion, ~0.003 Å^2 (Table III; ref 5).[15] Values of $\Delta\mathbf{U}_{obsd}(\text{Cu-O})$ cover a very much larger range, ~0–0.24 Å^2, i.e., they are up to 100 times as large. Since corresponding esd's are about the same for both, the values of $\Delta\mathbf{U}_{obsd}(\text{Cu-O})$ indicate chemically significant information about the disorder of the O atoms.

(15) The distribution of $[\Delta\mathbf{U}_{obsd}(\text{M-N}) - 0.003\ \text{Å}^2]/\sigma(\Delta\mathbf{U}_{obsd})$ is almost normal if five outliers (absolute ratio >3) are disregarded. One significant negative deviation is found for both [Cu24] and [Cu25]. These are discussed in connection with the exceptionally large values of $\mathbf{U}_{obsd}(\text{Cu-O2})$ found for these compounds and shown to be, at least partially, of physical origin. The negative deviations found for [Cu04] are most likely due to an inadequacy in the experiment (done at 165 K) since the data for the very same structure obtained at 298, 100, and 20 K ([Cu03], [Cu05], [Cu06]) do not show such deviations. The negative deviation for [Cu23] has no obvious reason.

Table V. Bibliography of $[Cu^{II}(LL)_2OXO]Y$ Complexes

(1) Walsh, A.; Walsh, B.; Murphy, B.; Hathaway, B. J. *Acta Crystallogr., Sect. B: Struct. Crystallogr. Cryst. Chem.* **1981**, *B37*, 1512–1520.
(2) Procter, I. M.; Stephens, F. S. *J. Chem. Soc. A* **1969**, 1248–1255.
(3) Simmons, C. J.; Clearfield, A.; Fitzgerald, W.; Tyagi, S.; Hathaway, B. J. *Inorg. Chem.* **1983**, *22*, 2463–2466.
(4) Simmons, C.; Clearfield, A.; Fitzgerald, W.; Tyagi, S.; Hathaway, B. J. *J. Chem. Soc., Dalton Trans.* **1983**, 189–190.
(5) Simmons, C. J.; Clearfield, A.; Fitzgerald, W.; Tyagi, S.; Hathaway, B. J. **1983**, unpublished results.
(6) Simmons, C. J.; Seff, K.; Clifford, F.; Hathaway, B. J. *Acta Crystallogr., Sect. C: Cryst. Struct. Commun.* **1983**, *C39*, 1360–1367.
(7) Kasempimolporn, V.; Tyagi, S.; Hathaway, B. J. **1980**, unpublished work.
(8) Chen, H. A.; Fackler, J. P. **1984**, private communication.
(9) Fereday, R. J.; Hodgson, P.; Tyagi, S.; Hathaway, B. J. *J. Chem. Soc., Dalton Trans* **1981**, 2070–2077.
(10) Nakai, H. *Bull. Chem. Soc. Jpn.* **1980**, *53*, 1321–1326.
(11) Hathaway, B. J. **1984**, private communication.
(12) Hathaway, B. J.; Ray, N.; Kennedy, D.; O'Brien, N.; Murphy, B. *Acta Crystallogr., Sect. B: Struct. Crystallogr. Cryst. Chem.* **1980**, *B36*, 1371–1377.
(13) Clifford, F.; Counihan, E.; Fitzgerald, W.; Seff, K.; Simmons, C. J.; Tyagi, S.; Hathaway, B. J. *J. Chem. Soc., Chem. Commun.* **1982**, 196–198.
(14) Fitzgerald, W.; Hathaway, B. J. *Acta Crystallogr., Sect. C: Cryst. Struct. Commun.* **1984**, *C40*, 243–245.
(15) Simmons, C. J.; Alcock, N. W.; Seff, K.; Fitzgerald, W.; Hathaway, B. J. **1984**, unpublished results.
(16) Fitzgerald, W.; Hathaway, B. J. *J. Chem. Soc., Dalton Trans.* **1985**, 141–149.
(17) Fitzgerald, W.; Hathaway, B. J. *J. Chem. Soc., Dalton Trans.* **1981**, 567–574.
(18) Escobar, C.; Wittke, O. **1984**, private communication.
(19) Escobar, C.; Wittke, O. *Acta Crystallogr., Sect. C: Cryst. Struct. Commun.* **1983**, *C39*, 1643–1646.

Figure 4 shows scatterplots of $\Delta U_{obsd}(Cu–O)$ vs. the difference in apparent distances $\langle \Delta d(Cu–O) \rangle$ for $[Cu^{II}(LL)_2ONO]^+$ and $[Cu^{II}(LL)_2CH_3COO]^+$ ions. Each compound contributes two points: $\Delta U_{obsd}(Cu–O1)$ at negative $\langle \Delta d(Cu–O) \rangle$ and $\Delta U_{obsd}(Cu–O2)$ at positive $\langle \Delta d(Cu–O) \rangle$. Even casual inspection of Figure 4 reveals the quadratic dependence postulated in eq 1. Both plots show a well-defined maximum at $\langle \Delta d(Cu–O) \rangle \approx 0$ with data points covering the entire range of structures from symmetric to very asymmetric. The maximum is lower for small $\Delta d(Cu–O)$ than for large $\Delta d(Cu–O)$, as expected from eq 1.

Along more quantitative lines, the coefficients in eq 2 have been calculated by linear regression including eight out of nine nitrite complexes (without [Cu07]) and seven out of nine acetate complexes (without [Cu24], [Cu25]). They are, for nitrite and acetate, respectively

$$\Delta U_{obsd} = 0.072\ (2) + 0.038\ (13)\langle \Delta d(Cu–O) \rangle - \langle \Delta d(Cu–O) \rangle^2\ [Å^2]$$

$$\Delta U_{obsd} = 0.131\ (6) + 0.046\ (23)\langle \Delta d(Cu–O) \rangle - \langle \Delta d(Cu–O) \rangle^2\ [Å^2]$$

The respective correlation coefficients are $r^2 = 0.90$ and 0.78. The four formate complexes are either symmetric or very asymmetric. The regression equation including all four compounds is

$$\Delta U_{obsd} = 0.194\ (6) + 0.037\ (18)\langle \Delta d(Cu–O) \rangle - \langle \Delta d(Cu–O) \rangle^2\ [Å^2]$$

with $r^2 = 0.97$. The three nitrato compounds are all very asymmetric, i.e., there are not enough data to calculate a meaningful regression equation.

The coefficients of the quadratic regressions conform with the models given in eq 1 and 2. The constants nicely reflect the trend in asymmetries $\Delta d(Cu–O)$, which are $\sim$0.24 Å for NO_2^-, $\sim$0.35 Å for CH_3COO^-, and $\sim$0.43 Å for $HCOO^-$. The coefficients of the linear term are consistently $\sim$0.04 Å. The coefficients of

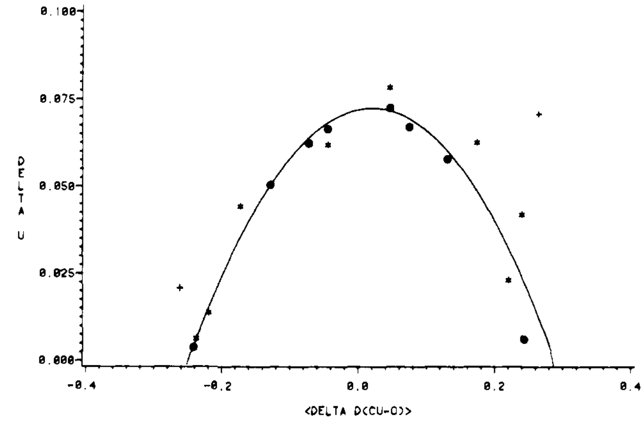

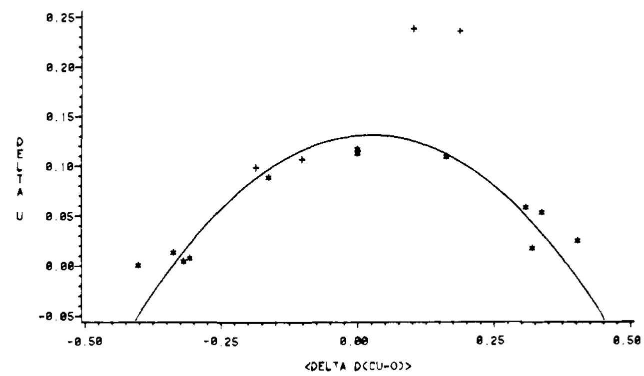

Figure 4. Scatterplot of $\Delta U_{obsd}(Cu–O)$ [$Å^2$] vs. $\langle \Delta d(Cu–O) \rangle$ [Å] for (top) $[Cu^{II}(LL)_2ONO]^+$ complexes (+, [Cu07]; *, [Cu03]–[Cu06], --- quadratic regression, see text); (bottom) $Cu^{II}(LL)_2CH_3COO]^+$ complexes (+, [Cu24], [Cu25]); --- quadratic regression, see text).

the quadratic term have been constrained to −1 to conform with eq 1 and 2. If a reasonable value for ΔU_s is assumed, $\sim$0.003 $Å^2$, ΔU_l is calculated to be 0.022, 0.031, and 0.037 $Å^2$ from the coefficients of the linear term. The maximum asymmetries calculated from eq 2 taking into account the constant terms ΔU_s and ΔU_l are 0.24, 0.34, and 0.42 Å in good agreement with the observed values (see above). Note also the linear correlation $\Delta U(Cu–O) = 0.003 + 0.04[d(Cu–O) - 2.0]$ $Å^2$ which might be of empirical value. On the basis of these findings it is predicted that for nitrate complexes $\Delta U_{obsd} \approx 0.10 + 0.04\ \langle \Delta d(Cu–O) \rangle - \langle \Delta d(Cu–O) \rangle^2$ [$Å^2$].

The root-mean-square deviations between ΔU_{obsd} and ΔU estimated from quadratic regressions are, respectively, 0.0080, 0.0217, and 0.0137 $Å^2$, several times larger than the root-mean-square standard deviations of $\sim$0.0040 $Å^2$. There are several possible reasons for the inability of the quadratic regression to reproduce ΔU_{obsd} to within their esd's: (1) variation of the nitrogen ligands, (2) inadequacy of harmonic (Gaussian) displacement parameters for a double minimum potential with atomic rms displacements as high as 0.43 Å, (3) limited resolution and other systematic errors in the data leading to some uncertainty in U_{obsd}, especially of the O atom.

Some remarks on the outliers excluded from the regression calculations are in order. In the series of NO_2^- complexes $[Cu(phen)_2ONO]BF_4$ ([Cu07], + in Figure 4) was excluded, as it is the only compound with a phenanthroline ligand. This is hardly a sufficient explanation for the deviation from the observed correlation, since for the CH_3COO complexes the phen compounds are not different from the bipy and bipyam compounds. It is, however, the only obvious difference to the remaining compounds. In the series of CH_3COO complexes the data sets [Cu24] and [Cu25] pertaining to measurements on $[Cu(phen)_2CH_3COO]ClO_4$ at 298 and 173 K were excluded. Both show values of $\Delta U_{obsd}(Cu–O2)$ which are too large by a factor of $\sim$2. Moreover the values of ΔU_{obsd}(Cu–N2) are significantly negative (Table IV). Qualitatively these observations may be explained as follows: The site symmetry of the cation is C_1, i.e., there is no reason that the positions of the Cu atoms in the disordered molecules I and II are the same (Figure 1). If we assume that the transition I $\rightleftarrows$ II is accompanied by a shift δ of Cu approximately in the direction of O2, the following relationship may be obtained

$$\Delta U_{dis}(\text{Cu–O2}) = [\Delta d^2(\text{Cu–O2}) - \langle \Delta d(\text{Cu–O2}) \rangle^2]\,[1 + \delta/\Delta d(\text{Cu–O2})]$$

$$\Delta U_{dis}(\text{Cu–N2}) = [\Delta d^2(\text{Cu–N2}) - \langle \Delta d(\text{Cu–N2}) \rangle^2]\,[1 - v/\Delta d(\text{Cu–N2})]$$

By using observed values for Δd, $\langle \Delta d \rangle$, and $\Delta U_{obsd} - 0.003$ Å^2 $\approx \Delta U_{dis}$, δ is calculated to be ~0.4 Å from ΔU_{obsd}(Cu–O2) and ~0.2 Å from ΔU_{obsd}(Cu–N2). The two estimates do not agree very well but at least they have the same sign and order of magnitude.

A similar analysis for the dependence of ΔU_{obsd}(Cu–N_{eq}) on $\langle \Delta d$(Cu–N)$\rangle$ for N1 and N2 does not give significant results because the value of ΔU_{dis}(Cu–N) estimated from Δd(Cu–N) is ~0.005 Å^2, approximately the same as the root-mean-square standard deviation of U_{obsd}(Cu–N) (~0.004 Å^2).

Conclusion

The data sets [CuO3] to [CuO6] all pertain to [Cu^{II}(bipy)$_2$ONO]NO_3 measured by diffractometry at 298, 165, 100, and 20 K. (⊛ in Figure 4). The site symmetry of Cu is C_1, the energy difference E between I and II (Figure 1) is ~150 cm^{-1}, and the population factor P therefore depends on T.[14] As Figure 4 shows the corresponding data points nicely follow the regression curve. This indicates that the energy barrier between I and II is sufficiently small to allow equilibration and that the disorder, at least for this compound, is dynamic rather than static. For the data sets [Cu24] and [Cu25] pertaining to [Cu^{II}phen$_2$$CH_3COO$]$ClO_4$ measured at 298 and 165 K the case for dynamic disorder is less convincing.

In summary, the variation in d(Cu–O) and ΔU_{obsd}(Cu–O) may be largely explained in terms of a simple geometrical model for the automerization between the two forms of the [Cu^{II}(LL)$_2$X]$^+$ ion (I, II, Figure 1). This provides additional support to the potential energy curve and the underlying geometrical model of the pseudo-Jahn–Teller distortion. Deviations from this model are either due to its simplistic nature or to the limited accuracy of U_{obsd}.

The present analysis is another example in a series of interpretations of ΔU_{obsd} values[5] from routine structure determinations. Other studies were concerned with Jahn–Teller distortions of $Cu^{II}N_6$ and $Mn^{III}F_6$ coordination octahedra,[5b,16] with spin changes in $Fe^{III}S_6$ coordination octahedra[5c] and with valence disorder in a binuclear N_4Mn^{III}–(μ-O)$_2$–$Mn^{IV}N_4$ complex.[17] These studies show that for crystal structure analysis of coordination compounds done with average accuracy values of ΔU_{obsd} in the range 0.2–0.003 Å^2 are amenable to chemical interpretation. For compounds containing first-row atoms only, ΔU_{obsd} as low as 0.001 Å^2 may still be chemically meaningful, if accurate diffraction data to high scattering angle are interpreted in terms of multipole models of the molecular electron density function.[18]

Acknowledgment. We appreciate the cooperation of Prof. C. J. Simmons and Prof. B. J. Hathaway in promptly providing unpublished data. We acknowledge the comments of a referee.

Supplementary Material Available: A table summarizing details of data collection and refinement (1 page). Ordering information is given on any current masthead page.

(16) Vedani, A. Ph.D. Thesis, University of Zürich, 1981.
(17) (a) Stebler, M.; Ludi, A.; Bürgi, H. B. *Inorg. Chem.* **1986**, *22*, 4743. (b) Stebler, M. Ph.D. Thesis, University of Bern, 1986.
(18) Bürgi, H. B., in preparation.

Alkyne Ligands as Two-Electron Donors in Octahedral d^6 Tungsten(0) Complexes: *fac*-$W(CO)_3$(dppe)(η^2-HC≡CR) and $W(CO)_2$(dppe)(DMAC)$_2$

K. R. Birdwhistell, T. L. Tonker, and J. L. Templeton*

Contribution from the W. R. Kenan, Jr. Laboratory, Department of Chemistry, University of North Carolina, Chapel Hill, North Carolina 27514. *Received July 3, 1986*

Abstract: Three labile terminal alkyne adducts of tungsten(0), *fac*-$W(CO)_3$(dppe)(η^2-HC≡CR) (dppe = $Ph_2PCH_2CH_2PPh_2$; R = H, *n*-Bu, and Ph) have been synthesized from *fac*-$W(CO)_3$(dppe)(acetone). Chemical and spectroscopic properties indicate that the alkyne ligand is weakly bound in these octahedral d^6 monomers. Recognition of an unfavorable 2-center-4-electron repulsion between the filled alkyne $\pi_\perp$ orbital and a filled metal $d\pi$ orbital helps to rationalize the observed chemistry. Internal alkyl and aryl alkynes do not yield clean products under similar reaction conditions, but the electron poor ester substituted alkyne DMAC (DMAC = dimethylacetylenedicarboxylate) forms $W(CO)_2$(dppe)(DMAC)$_2$. A single-crystal X-ray study of this complex confirmed the trans alkyne–cis dicarbonyl geometry anticipated from spectroscopic data [space group $P\bar{1}$, a = 11.51 (1) Å, b = 18.90 (1) Å, c = 10.27 (1) Å, α = 102.74 (6)°, β = 107.90 (8)°, γ = 79.95 (8)°, Z = 2, R = 0.035, R_w = 0.047 for 6000 unique data with $I > 3\sigma(I)$]. The two trans alkyne ligands are orthogonal to one another with each alkyne eclipsing one of the two P–W–C vectors of the equatorial $W(CO)_2$(dppe) unit. Dynamic ^{1}H NMR studies reveal a barrier of 17.7 kcal/mol for averaging the two ends of each DMAC ligand, presumably by an alkyne rotation process. The role of alkyne ester substituents in promoting $d\pi$ to $\pi_\parallel^*$ backbonding *and* delocalizing $\pi_\perp$ alkyne electrons away from $d\pi$ metal electron density is discussed. These results help to rationalize three general features of transition-metal alkyne chemistry: (i) two-electron donor DMAC analogues of metal–olefin complexes are common; (ii) d^6 metal octahedra promote isomerization of terminal alkyne ligands to vinylidenes, and (iii) terminal and dialkyl alkyne ligands prefer to bind to high oxidation state metals having at least one vacant $d\pi$ orbital.

Numerous octahedral molybdenum and tungsten d^4 monomers contain one[1] or two[2] tightly bound alkyne ligands. The d^2 configuration is also well represented among octahedral molybdenum[3] and tungsten[4] complexes containing an alkyne ligand. Both of

 © 1987 American Chemical Society